



Bertram, J., Tanwear, A., Rodriguez, A., Paterson, G., McVitie, S. and Heidari, H.
(2019) Spin-Hall Nano-Oscillator Simulations. In: IEEE Sensors 2019, Montreal, QC,
Canada, 27-30 Oct 2019, ISBN 9781728116341.

There may be differences between this version and the published version. You are
advised to consult the publisher's version if you wish to cite from it.

<http://eprints.gla.ac.uk/192778/>

Deposited on: 12 August 2019

Enlighten – Research publications by members of the University of Glasgow
<http://eprints.gla.ac.uk>

Spin-Hall Nano-Oscillator Simulations

Jon Bertram¹, Asfand Tanwear¹, Aurelio Rodriguez², Gary Paterson², Stephen McVitie² and Hadi Heidari¹

¹ Microelectronics Lab (meLAB), School of Engineering, University of Glasgow, G12 8QQ, UK

² Materials and Condensed Matter Group, School of Physics, University of Glasgow, G12 8QQ, UK

hadi.heidari@glasgow.ac.uk

Abstract— A spin-Hall nano-oscillator (SHNO) is a type of spintronic oscillator that shows promising performance as a nanoscale microwave source and for neuromorphic computing applications. Within such nanodevices, a non-ferromagnetic layer in the presence of an external magnetic field and a DC bias current generates an oscillating microwave voltage. For developing optimal nano-oscillators, accurate simulations of the device's complex behaviour are required before fabrication. This work simulates the key behaviour of a nanoconstriction SHNO as the applied DC bias current is varied. The current density and Oersted field of the device have been presented, the magnetisation oscillations have been clearly visualised in three dimensions and the spatial distribution of the active mode determined. These simulations allow designers a greater understanding and characterisation of the device's behaviour while also providing a means of comparison when experimental results are generated.

Keywords — FEM Simulation, Micromagnetic Simulation, Magnetic Oscillations, Spin-Hall Nano-Oscillator, SHNO.

I. INTRODUCTION

Having only recently been discovered spintronic oscillators overcome the typical sensitivity of nanoscale devices to external factors by being magnetically operated. These devices can then operate as microwave sources or as a neuron in neural network applications. Spintronic oscillators are particularly suited for neuromorphic computing systems due to the non-linear oscillatory behaviour of the device's magnetisation and their ability to synchronise magnetically or electrically with other identical devices [1]. By utilising a single spintronic oscillator to emulate a neuron, the low power inefficiencies and space requirements of CMOS architecture [2] can be overcome by removing the need for multitudes of transistors required to effectively replicate a neuron's behaviour.

A Spin Torque Nano Oscillator (STNO) is one such device that has in recent years been successfully applied to neural network applications, more specifically for vowel recognition [3] [4]. Spin Hall Nano Oscillators (SHNO) share similar operation to STNOs but bring with them substantial benefits in allowing direct optical access for easier characterisation of the device's behaviour and in a reduced operational current.

An SHNO device consists of a ferromagnetic (FM) and nonferromagnetic (NFM) bilayer structure whereby the generation of spin current results in a spin torque present in the FM layer, which can then ensure steady precession of the magnetisation. This operation is achieved by the application of a DC current to the NFM layer that is then converted to pure spin current flowing in the transverse direction by the spin Hall effect (SHE). The pure spin current then flows through the NFM/FM interface and exerts a spin transfer torque (STT) on the magnetisation of the FM layer. If current densities are significant enough to generate a substantial Spin Transfer Torque the damping action of the magnetisation can be overcome, and the magnetisation can achieve a steady unchanging precession

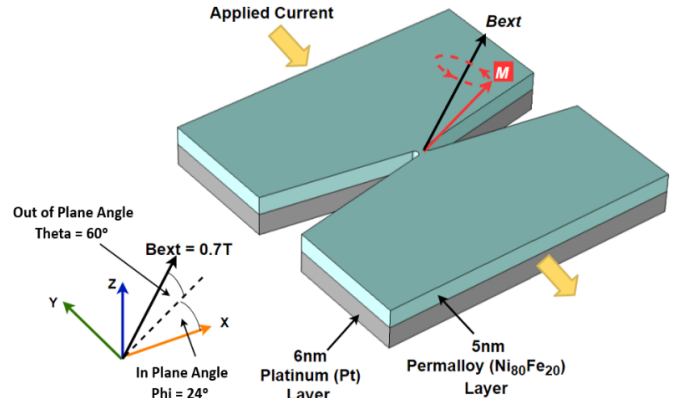


Fig 1. The nanoconstriction SHNO device structure.

known as an auto-oscillation (AO) mode. Through the Anisotropic Magnetoresistance effect (AMR) effect this can then be converted to a microwave voltage.

In recent years the nanoconstriction (NC) geometry (Fig. 1) has shown the most promise of an eventual neural network application [5] [6] [7] [8]. The constricted region produces extremely high local current densities and subsequent STTs at operational currents in the mA range while also allowing for direct optical access to the active area. These SHNO devices have demonstrated mutual synchronisation between multiple devices which is a key requirement for neural network applications. Multiple NC SHNOs have been synchronised across distances up to $4\mu\text{m}$ [1], with applied magnetic fields as small as 30mT [9], in stacked arrangements [10] and in arrays of 64 synchronised devices [11].

Using a combination of COMSOL Multiphysics [12] and MUMAX3 [13] (Fig. 2) this paper presents a method for simulating SHNO device behaviour with results comparable to those previously demonstrated [7]. In the existing literature the magnetisation oscillations of the system are yet to be clearly detailed. Here the magnetisation oscillations are presented for a selection of currents while the spatial distribution of the auto-oscillation mode across the device is also demonstrated. This work thereby effectively introduces SHNO behaviour by visualising the oscillations that drive device operation.

II. STRUCTURE AND MODELLING

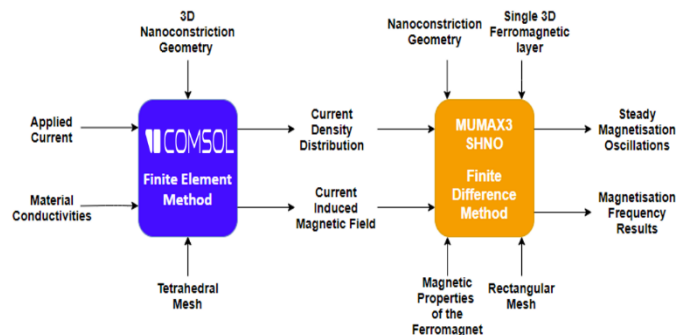


Fig. 2. COMSOL to MUMAX simulation workflow.

A. COMSOL Structure

COMSOL was used to calculate the current density distribution and the subsequent current-induced magnetic (Oersted) field across the SHNO. The modelled device consisted of a 4 μm by 4 μm Platinum/Permalloy bilayer with thicknesses of 6nm and 5nm respectively. A 20nm wide nanoconstriction was defined in the centre of the device with an opening angle of 22° and a 50nm radius of curvature. An in-plane DC current of 1.2mA was applied to the platinum layer and a tetrahedral mesh with minimum element sizing of 0.2nm was defined. Standard conductivity values of 8.9 MS/m for platinum and 1.74 MS/m for permalloy were also defined. In order to generate a solution using the “electric and magnetic fields” interface the device was encapsulated by a cube of air.

The current density distribution was taken in-plane at the mid-point of the platinum layer as this value determines the spin current and corresponding spin torque in the ferromagnetic layer. The Oersted field value was taken from the mid-point of the permalloy layer. Once calculated at a single applied current, the current can later be varied in MUMAX due to the linear relationships between current and its distributions.

B. MUMAX Structure

The calculated distribution values were then inserted into MUMAX3 to simulate the complex magnetic behaviour of the SHNO device. These values are estimated on the 2560nm \times 2560nm \times 5nm rectangular MUMAX mesh before this mesh is discretised into a grid of 1024 \times 1024 \times 1 cells each with dimensions of 2.5nm \times 2.5nm \times 1nm. A greyscale 1024 \times 1024 pixels image mask was used to implement the NC geometry while the material parameters were taken from previously published experimental data [7] [14] and can be seen in Table 1.

Lambda here determines the degree of angular dependency of the generated Spin Orbit Torque on the relative orientation between the magnetisation direction and spin polarisation direction [14]. Here we set this to 1 to remove any angular dependency from the simulation.

Table 1. MUMAX Material Parameters.

Parameter (Unit)	Value
Saturation Magnetisation M_s (A/m)	589000
Exchange Thickness, A (pJ/m)	12
Gilbert Damping, α	0.02
Spin-Hall Angle, Θ_{SH}	0.07
Lambda, Λ	1
Gyromagnetic Ratio, γ (GHz/T)	29.53

The spin-polarisation direction was set equal to the negative x direction and assumed uniformly antiparallel to the x-axis, $m_p = -1$. Zhang-Li torque was neglected due to the majority of the current flowing in the Pt layer and the contribution of any field-like spin-transfer torques (e') was ignored due to their small magnitudes in comparison to the damping-like contributions [15]. An external magnetic field of 0.7T was applied to the device, in addition to the Oersted field, with an in-plane angle of 24° and an out of plane angle of 60° (Fig. 1).

The magnetisation dynamics of the system were therefore calculated from the following modified Landau-Lifshitz-Gilbert-Slonczewski (LLGS) equation:

$$\frac{\partial \mathbf{M}}{\partial t} = \gamma \frac{1}{1 + \alpha^2} (\mathbf{m} \times \mathbf{B}_{eff} + \alpha (\mathbf{m} \times (\mathbf{m} \times \mathbf{B}_{eff}))) + \beta \frac{\epsilon - \alpha \epsilon'}{1 + \alpha^2} (\mathbf{m} \times (\mathbf{m}_P \times \mathbf{m})) \quad (1)$$

$$\beta = \frac{j_z \hbar}{M_{sat} e d} \quad (2)$$

$$\epsilon = \frac{\theta_{SH} \Lambda^2}{(\Lambda^2 + 1) + (\Lambda^2 - 1)(\mathbf{m} \cdot \mathbf{m}_P)} \quad (3)$$

Where (1) describes how the magnetisation oscillates before achieving auto-oscillation.

III. SIMULATION RESULTS AND DISCUSSION

A. COMSOL Distributions @ $I = 1.2\text{mA}$

A 100nm NC width geometry was constructed to verify the COMSOL methodology against previous results [14] before the following current density and Oersted field distributions were calculated. Fig. 3a and Fig. 3b both show the effect the NC has on SHNO operation as the crucial factors that influence the device’s behaviour are both significantly increased.

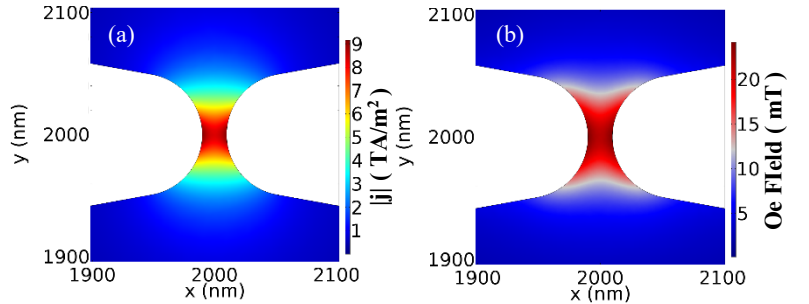


Fig 3. 20nm NC Distributions at 1.2mA
(a) Current Density (b) Current-induced (Oersted) magnetic field

B. Micromagnetic Simulation in MUMAX3

Fig. 4a and Fig. 4b demonstrate how the magnetisation of the system in the local NC area behaves as it achieves auto-oscillation. Once the device is excited at 1ns, by the addition of the current and Oersted field, the magnetisation begins to noticeably oscillate. At 0.6mA the amplitude of this transient oscillation builds until the magnetisation achieves auto oscillation, while at 1.2mA the amplitude instead decreases before entering the auto-oscillation mode. At both currents the auto-oscillation regime is achieved in a similar time frame of roughly 11ns despite the substantial difference in behaviour. The amplitude of the auto-oscillations was noted to behave non-linearly which is a crucial factor in neural network applications. A reduction in the amplitude of oscillations was observed between 1.1mA and 1.2mA suggesting a breakdown in device behaviour at high currents.

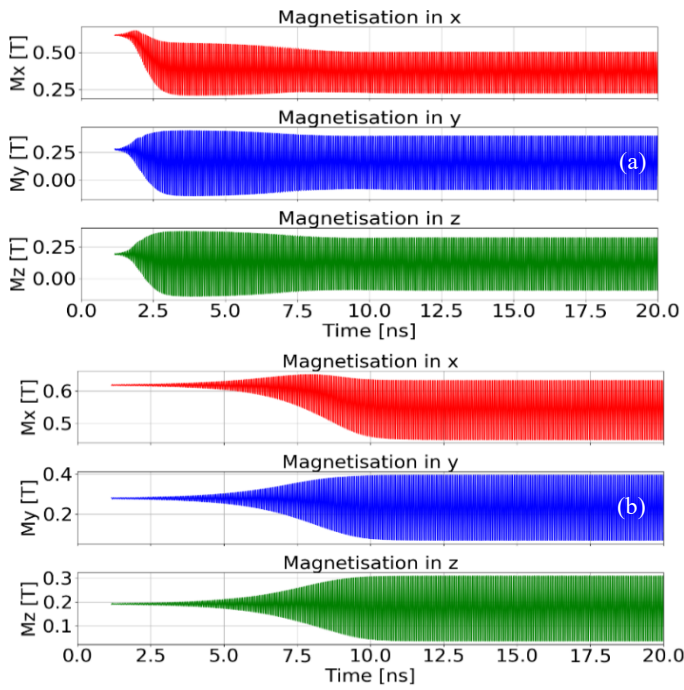


Fig 4. Magnetisation Oscillations in x, y and z
(a) $I = 0.6\text{mA}$ (b) $I = 1.2\text{mA}$

Fig. 5 show how the magnetisation in the local area is represented in three-dimensional space. The magnetisation in both cases can be seen to rotate around a fixed direction defined by the applied external magnetic field with the eventual auto-oscillation rotation denoted by the orange and red lines.

After the frequency of the auto-oscillation mode is calculated by taking the fast Fourier transform of the magnetisation across each cell, the spatial distribution of the active mode can be plotted. With an applied current of 0.6mA the distribution in Fig. 6a at a frequency of 17.73GHz is produced. The active mode is tilted due to the presence of the demagnetising field in the device and this tilt direction can be varied using the sign of the spin-Hall angle, the polarisation direction of the spin current or the direction of the applied current. The mode is present in a mostly uniform manner in the NC centre apart from two more prominent bands that have detached from the centre. This distribution is mostly symmetric and extends 200nm along the applied current path. At the increased current of 1.2mA and a frequency of 17.81GHz the distribution depicted in Fig. 6b is determined. This distribution varies substantially compared to the lower current result in that the mode is no longer uniformly distributed in the centre. Instead the mode exists most prominently in the two bands at distances of 40nm and 50nm in the positive and negative y direction

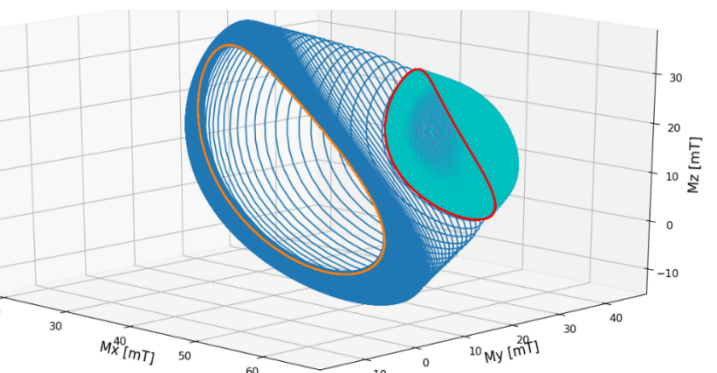
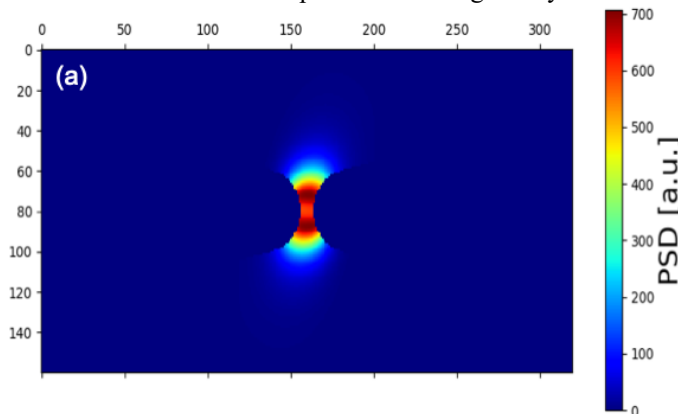


Fig 5. 3D Magnetisation Rotations, the secondary colour denotes the Auto-oscillation mode
Blue/Orange ($I = 1.2\text{mA}$), Cyan/Red ($I = 0.6\text{mA}$)

respectively. The mode now exhibits significant asymmetry due to the increase in the magnitude of the Oersted field and extends a total distance of 250nm along the applied current path.

When compared to simulated distributions of the active mode that have been previously published [7] the most substantial difference is in the presence of substantial asymmetry in the 1.2mA result. However, decreasing the current slightly to 1.1mA almost completely removes this asymmetry in the result again suggesting that the device behaviour breaks down above this applied current. These results also differ in the banded areas where the active mode is most prominent, but this could be due to the increased resolution (cell size decreased from $3.9\text{nm} \times 3.9\text{nm} \times 1\text{nm}$ to $2.5\text{nm} \times 2.5\text{nm} \times 1\text{nm}$) used in the simulated NC area.

IV. CONCLUSION

In summary a state-of-the-art NC SHNO has been simulated using a combination of COMSOL and MUMAX3. This simulation presents how an applied current in the mA range results in substantial current densities and Oersted field magnitudes in the NC area. These factors have a significant effect on the operation of an SHNO and are therefore crucial in achieving an accurate simulation. Through calculating these distributions, the complete complex behaviour of the SHNO device was simulated and the magnetisation dynamics assessed. The magnetisation in the local NC area achieves auto oscillation differently depending on the magnitude of the applied current as the magnitude of the STT varies. However, differences in the applied current do not affect the time taken to achieve auto-oscillation. The established method allows for easy evaluation of different materials and geometries before device fabrication while in visualising how the magnetisation evolves in three dimensions the behaviour of an SHNO has been more clearly visualised than ever before.

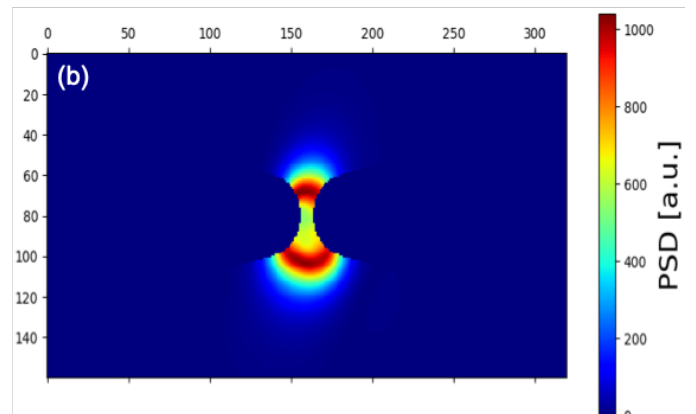


Fig 6. Spatial Distribution of the Auto-oscillation mode (a) $I = 0.6\text{mA}$, Frequency = 17.73GHz and (b) $I = 1.2\text{mA}$, Frequency = 17.81GHz .

REFERENCES

- [1] A. A. Awad, P. Dürrenfeld, A. Houshang, M. Dvornik, E. Iacocco and R. K. a. Å. J. Dumas, “Long-range mutual synchronization of spin Hall nano-oscillators,” *Nature*, vol. 13, p. pp 292–299, 2017.
- [2] J. Grollier, D. Querlioz and D. S. Mark, “Spintronic Nanodevices for Bioinspired Computing,” *Proceedings of the IEEE*, vol. 104, no. 10, pp. 2024-2040, October 2016.
- [3] J. Torrejon, M. Riou, F. A. Araujo, S. Tsunegi, G. Khalsa, D. Querlioz, P. Bortolotti, V. Cros, K. Yakushiji, A. Fukushima, H. Kubota, S. Yuasa, M. D. Stiles and J. Grollier, “Neuromorphic computing with nanoscale spintronic oscillators,” *Nature*, vol. 547, pp. 428-432, July 2017.
- [4] M. Romera, P. Talatchian, S. Tsunegi and F. A. Abreu Araujo, “Vowel recognition with four coupled spin-torque nano-oscillators,” *Nature*, vol. 563, p. 230, 8 November 2018.
- [5] V. Demidov, S. Urazhdin, A. Zholud, A. V. Sadovnikov and S. O. Demokritov, “Nano-constriction based Spin Hall nano oscillator,” *Applied Physics Letters*, vol. 105, p. 17, 2014.
- [6] M. Zahedinejad, A. A. Awad, P. Durrenfeld, A. Houshang and Y. Yin, “Current Modulation of Nanoconstriction Spin-Hall Nano-Oscillators,” *IEEE Magnetism Letters*, vol. 8, p. no. 3704804, 2017.
- [7] P. Dürrenfeld, A. A. Awad, A. Houshang, R. K. Dumas and J. Åkerman, “A 20 nm spin Hall nano-oscillator,” *Nanoscale*, vol. 9, no. 3, pp. 1285-1891, 2017.
- [8] B. Divinskiy, V. E. Demidov, A. Kozhanov, A. B. Rinkevich and S. O. Demokritov, “Nanoconstriction spin-Hall oscillator with perpendicular magnetic anisotropy,” *Applied Physics Letters*, vol. 111, p. no . 032405, 2017.
- [9] H. Mazraati, “Linear, Non-Linear, and Synchronizing Spin Wave Modes in Spin Hall Nano-Oscillators,” KTH Royal Institute of Technology, Stockholm, 2018.
- [10] K. D. Hyung and S. Mincheol, “Phase difference dependence of output power in synchronized stacked spin Hall nano-oscillators,” *Journal of Physics: Condensed Matter*, vol. 30, no. 28, p. no. 284001, 2018.
- [11] M. Zahedinejad, A. A. Awad, S. Muralidhar, R. Khymyn, H. Fulara, H. Mazraati and M. a. Å. J. Dvornik, “Two-dimensional mutual synchronization in spin Hall nano-oscillator arrays,” *Preprint*, December 2018.
- [12] “<https://www.comsol.com/>,” [Online].
- [13] A. Vansteenkiste, J. Leliaert, M. Dvornik, M. Helsen, F. Garcia-Sanchez and B. V. Waeyenberge, “The Design and Verification of Mumax3,” *AIP Advances* 4, no. 107133, 2014.
- [14] M. Dvornik, A. A. Ahmad A. Awad and J. Åkerman, “Origin of Magnetization Auto-Oscillations in Constriction-Based Spin Hall Nano-Oscillators,” *Physical Review Applied*, vol. 9, no. 1, p. 014017, 2018.
- [15] T. Nan, S. Emori, C. T. Boone, X. Wang, T. M. Oxholm, J. G. Jones, B. M. Howe, G. J. Brown and N. X. Sun, “Comparison of spin-orbit torques and spin pumping across NiFe/Pt and NiFe/Cu/Pt interfaces,” *Physical Review B*, vol. 91, no. 21, p. 214416, June 2015.
- [16] R. Nair, “Evolution of Memory Architecture,” *Proceedings of the IEEE*, vol. 103, no. 8, pp. 1331-1345, August 2015.
- [17] G. Indiveri and S.-C. Liu, “Memory and Information Processing in Neuromorphic Systems,” *Proceedings of the IEEE*, vol. 103, no. 8, pp. 1379-1397, 2015.
- [18] S. Zuo, K. Nazarpur and H. Heidari, “Device Modelling of MgO-barrier tunnelling magnetoresistors for hybrid spintronic-CMOS,” *IEEE Electron Device Letters*, vol. 39, pp. 1784-1787, 2018.
- [19] S. Zuo, R. Ghannam and H. Heidari, “Spintronic Nanodevices for Neuromorphic Sensing Chips,” 2018.